J. Fluid Mech. (1990), *vol.* 213, *pp.* 465–477
Printed in Great Britain

Flows emerging from a nozzle and falling under gravity

By FRÉDÉRIC DIAS[1] AND JEAN-MARC VANDEN-BROECK[2]

[1] Department of Mathematical Sciences, Worcester Polytechnic Institute, Worcester, MA 01609, USA

[2] Department of Mathematics and Center for the Mathematical Sciences, University of Wisconsin-Madison, Madison, WI 53705, USA

(Received 30 May 1989 and in revised form 27 September 1989)

Steady two-dimensional free-surface flows of an inviscid and incompressible fluid emerging from a nozzle and falling under gravity are calculated numerically. The nozzle is aimed at an angle β above the horizontal. It is shown that there are flows for which the fluid falls down along the underside of the nozzle and other flows which split into two sheets. The latter flows occur for each value of β when the Froude number F is greater than a critical value. Local solutions are constructed to describe the limiting behaviour of the flows as $F \rightarrow 0$ and as $F \rightarrow \infty$.

1. Introduction

When a stream of fluid emerges from a two-dimensional nozzle aimed at an angle β above the horizontal, the stream rises to a maximum height and then falls under gravity. When the angle β is close to $\frac{1}{2}\pi$ (i.e. the nozzle is almost vertical), the fluid splits into two jets (see figure 1*a*). On the other hand, when the angle β is sufficiently small, the fluid falls to one side, for example down along the underside of the nozzle as is shown in figure 6. We shall calculate these solutions numerically by assuming that the flow is steady, irrotational and two-dimensional and that the fluid is incompressible and inviscid. Similar numerical solutions were obtained recently by Goh & Tuck (1985) for waterfall flows emerging between horizontal plates and by Tuck (1987) for the waterfall from a slit in a vertical wall.

We shall see that the solutions are determined by the angle β and by the Froude number

$$F = \frac{U}{(gL)^{\frac{1}{2}}}. \tag{1}$$

Here g is the acceleration due to gravity, L the width of the nozzle and U the velocity far inside the nozzle. Our results show that there is a curve $F = F(\beta)$ (see figure 9) which separates the (β, F)-plane into two regions: the region above the curve corresponds to the solutions with two jets while the region below the curve corresponds to the solutions in which the fluid falls along the underside of the nozzle.

The problem is formulated in §2 and the results are presented in §§2–5. In §2, we present the solutions with two jets. In §3, we consider the asymptotic behaviour of the flow as $F \rightarrow \infty$. We show that the limiting flow as $F \rightarrow \infty$ can be viewed as the flow due to a source placed at the top of an inclined wall. A one-parameter family of solutions is presented. It includes as a particular case a solution previously computed by Mekias & Vanden-Broeck (1989). In §4, we present the solutions with only one

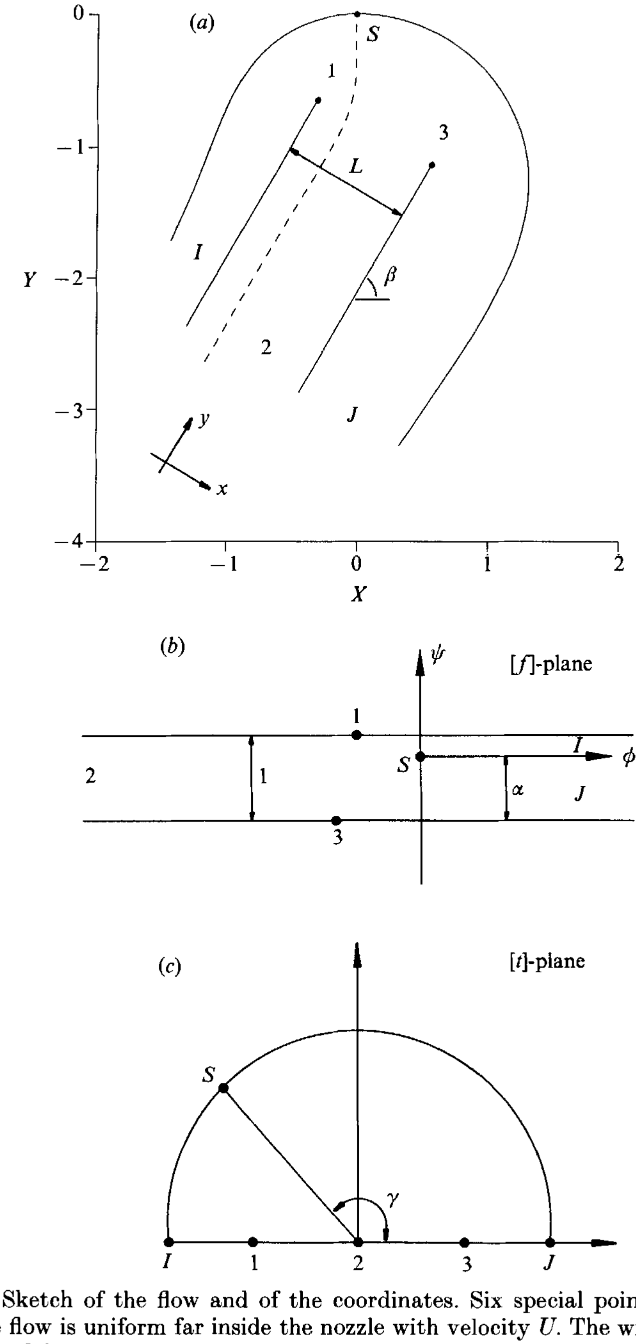

FIGURE 1. (*a*) Sketch of the flow and of the coordinates. Six special points are labelled on the boundary. The flow is uniform far inside the nozzle with velocity U. The width of the nozzle is L. The inclination of the nozzle with the horizontal is β. The free-surface profile is a computed solution for $\beta = 60°$ and $F = 3.0$. The vertical scale is the same as the horizontal scale. The broken line is the dividing streamline and S is the stagnation point. (*b*) The complex potential plane. The images of the six points are shown. (*c*) The complex [t]-plane. The images of the six points are shown.

sheet. Finally, in §5, we consider the limit as $F \to 0$. We show that the solutions near the lips of the nozzle are described by the 'pouring flows' calculated by Vanden-Broeck & Keller (1986). In addition, a solution with two jets each with two free surfaces is presented.

2. Flows which split into two jets

We consider the steady irrotational flow of an incompressible inviscid fluid emerging from a nozzle and falling under gravity. We assume that the flow splits into two jets (see figure 1*a*) and that both jets touch the outside of the nozzle. The nozzle has an inclination β with the horizontal, ranging from $\beta = 0$ (the nozzle is horizontal) to $\beta = \frac{1}{2}\pi$ (the nozzle points vertically upward). Two systems of orthonormal coordinates are defined: (X, Y) with X horizontal and Y vertical; and (x, y) with y along the direction of the nozzle. Gravity acts in the negative Y-direction. The amount of flow emerging from the nozzle is

$$Q = UL. \tag{2}$$

The pressure is assumed to be constant on the free surface so that Bernoulli's equation yields

$$\tfrac{1}{2}(u^2+v^2)+gY = \text{constant on free surface.} \tag{3}$$

Here u and v are the x- and y-components of the fluid velocity. The problem is non-dimensionalized by taking L as the unit length and U as the unit velocity. The discharge is now unity. In terms of the dimensionless variables, the condition (3) becomes

$$\tfrac{1}{2}(u^2+v^2)+\frac{1}{F^2}(y\sin\beta - x\cos\beta) = \text{constant on free surface.} \tag{4}$$

We denote the velocity potential by $\phi(x,y)$ and the stream function by $\psi(x,y)$. In addition we introduce the complex variables $z = x+\mathrm{i}y$ and $f = \phi+\mathrm{i}\psi$. The flow domain in the $[f]$-plane is shown in figure 1(*b*). It is an infinite strip of height 1 with a slit starting at the point S where the flow separates and extending to $+\infty$. This slit represents the free surface. The bottom of the strip represents the right side of the nozzle and the top of the strip the left side of the nozzle. The amount of fluid α falling down along the underside of the nozzle is measured by the height between the bottom of the strip and the slit.

We transform the domain occupied by the fluid in the $[f]$-plane into the upper half of the unit disk in the $[t]$-plane so that the points I, 2 and J are mapped into the points -1, 0 and 1 (see figure 1*c*). The left side of the nozzle goes onto $[-1,0]$, the right side onto $[0,1]$ and the free surface onto the upper half-unit circle. We denote the images of the points 1, 3 and S by t_1, t_3 and $\mathrm{e}^{\mathrm{i}\gamma}$. The transformation from the $[f]$-plane to the $[t]$-plane can be written in differential form as

$$\frac{\mathrm{d}f}{\mathrm{d}t} = -\frac{1}{\pi}\left[\frac{2t\cos\gamma-(1+t^2)}{t(1-t^2)}\right]. \tag{5}$$

It is easy to show that α and γ are related by

$$\alpha = \tfrac{1}{2}(1-\cos\gamma). \tag{6}$$

We introduce the hodograph variable

$$\zeta(z) = \frac{\mathrm{d}f(z)}{\mathrm{d}z} = u-\mathrm{i}v. \tag{7}$$

The problem is now to find ζ as an analytic function of t satisfying (4) and the kinematic boundary conditions on the real diameter $t \in [-1,1]$. Points on the upper half-unit circle (i.e. on the free surface) are represented by $t = e^{i\sigma}$, $\sigma \in [0,\pi]$. Next we differentiate (4) with respect to σ. This yields

$$(uu_\sigma + vv_\sigma) + \frac{1}{F^2}(y_\sigma \sin\beta - x_\sigma \cos\beta) = 0. \tag{8}$$

Substituting $t = e^{i\sigma}$ in (5) and using (7) we find after some algebra

$$\frac{\partial y}{\partial \sigma} = \frac{1}{\pi}\left(\frac{\cos\gamma - \cos\sigma}{\sin\sigma}\right)\frac{v}{u^2+v^2} \quad \text{and} \quad \frac{\partial x}{\partial \sigma} = \frac{1}{\pi}\left(\frac{\cos\gamma - \cos\sigma}{\sin\sigma}\right)\frac{u}{u^2+v^2}. \tag{9}$$

Inserting (9) in (8), we obtain

$$uu_\sigma + vv_\sigma + \frac{1}{\pi F^2}\left(\frac{\cos\gamma - \cos\sigma}{\sin\sigma}\right)\left[\frac{v\sin\beta - u\cos\beta}{u^2+v^2}\right] = 0. \tag{10}$$

At both extremities of the nozzle, the velocity of the fluid is infinite and ζ must have singularities at these points. The appropriate singularities are

$$\zeta \sim (t-t_1)^{-1} \quad \text{as} \quad t \to t_1 \tag{11}$$

$$\zeta \sim (t-t_3)^{-1} \quad \text{as} \quad t \to t_3. \tag{12}$$

At the point S where the flow separates, the velocity vanishes and the appropriate behaviour for ζ is

$$\zeta \sim t - e^{i\gamma} \quad \text{as} \quad t \to e^{i\gamma}. \tag{13}$$

The singularities at I and J are jet-type singularities (see Birkhoff & Carter 1957 and Vanden-Broeck & Keller 1986 for details) and can be combined as

$$\zeta \sim [-\ln(1-t^2)]^{\frac{1}{3}} \quad \text{as} \quad t \to \pm 1. \tag{14}$$

We now define the function $\Omega(t)$ by the relation

$$\zeta(t) = -i(1+t^2-2t\cos\gamma)\left(\frac{1-tt_3}{t-t_3}\right)\left(\frac{1-tt_1}{t-t_1}\right)\frac{[-\ln c(1-t^2)]^{\frac{1}{3}}}{[-\ln c]^{\frac{1}{3}}}t_1 t_3 e^{\Omega(t)}. \tag{15}$$

The function $\Omega(t)$ is analytic for $|t| < 1$ and continuous for $|t| \leqslant 1$. It can be expanded in a power series

$$\Omega(t) = \sum_1^\infty a_n t^n. \tag{16}$$

In (15), c is a constant, which we choose to be such that $[-\ln c(1-t^2)]^{\frac{1}{3}}$ is positive for $-1 < t < 1$. We chose $c = 0.2$. We checked that the computed values of ζ evaluated from (15) do not depend on the value of c chosen. From (15), it is easy to show that $\zeta(0) = -i$, i.e. the uniform velocity at 2 is 1.

The coefficients a_n are determined by collocation. To do so we truncate the infinite series in (16) after $N-3$ terms and we introduce the $N-1$ mesh points

$$\sigma_M = \frac{\pi}{N-1}(M-\tfrac{1}{2}), \quad M = 1, \ldots, N-1. \tag{17}$$

By using (15) we obtain the values of u, v, u_σ and v_σ at the points σ_M in terms of the coefficients a_n. Substituting these expressions into (8) at the points σ_M we obtain $N-1$ nonlinear algebraic equations for the N unknowns $t_1, t_3, a_n (1 \leqslant n \leqslant N-3)$ and γ. The Nth equation is obtained by imposing the constraint that the two extremities 1 and

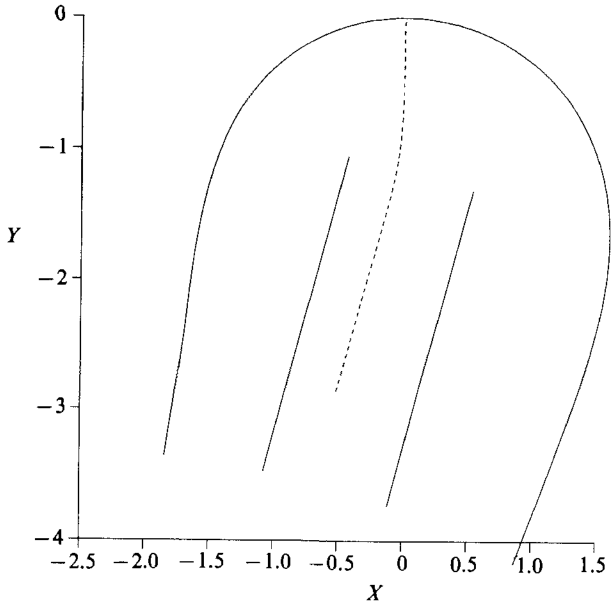

FIGURE 2. Same as figure 1 (*a*) with $\beta = 75°$ and $F = 5.0$. The broken line represents the dividing streamline. For this particular example, 61 % of the flow goes to the right.

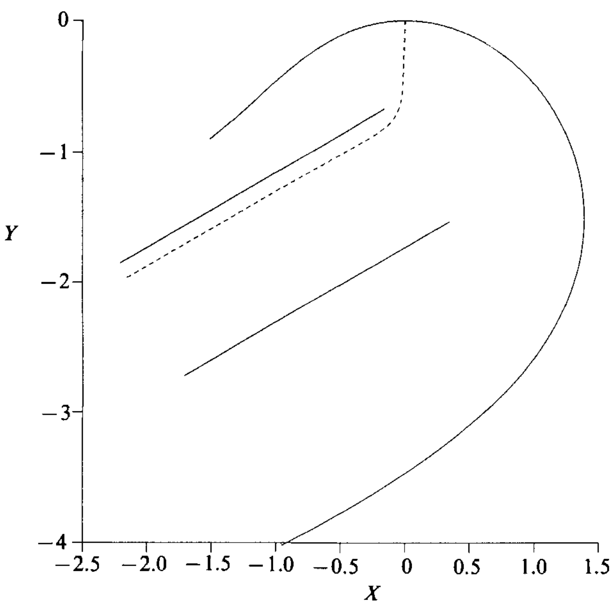

FIGURE 3. Same as figure 2 with $\beta = 30°$ and $F = 5.0$. 87 % of the flow goes to the right.

3 of the nozzle have the same y, i.e. $y_1 = y_3$. The coordinates of 1 and 3 are obtained by integrating numerically the equation

$$\frac{\mathrm{d}z}{\mathrm{d}t} = \left(\frac{1}{\zeta}\right)\frac{\mathrm{d}f}{\mathrm{d}t}. \tag{18}$$

This system of N nonlinear equations with N unknowns is solved by Newton's method for given values of F and β. The DN2QNF package of the IMSL library was

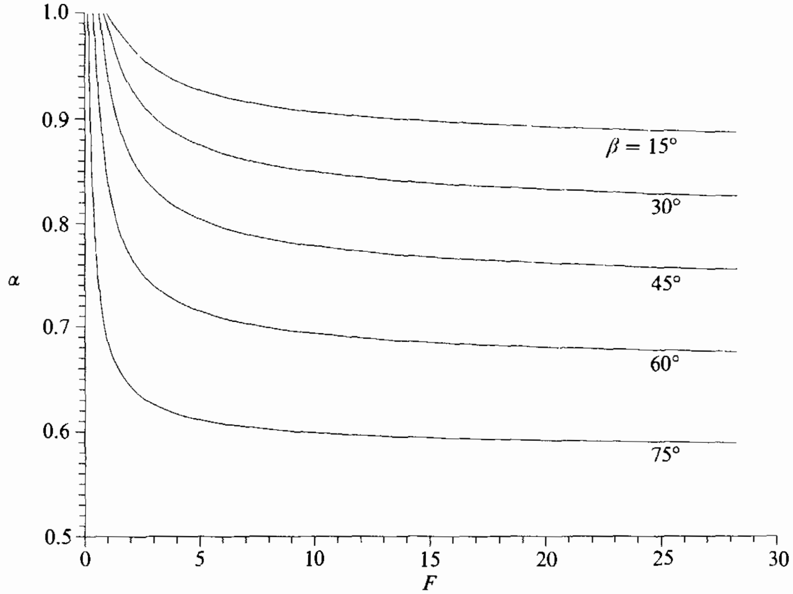

FIGURE 4. Values of the amount α of water falling down on the right versus the Froude number F, for various values of the inclination β of the nozzle with the horizontal.

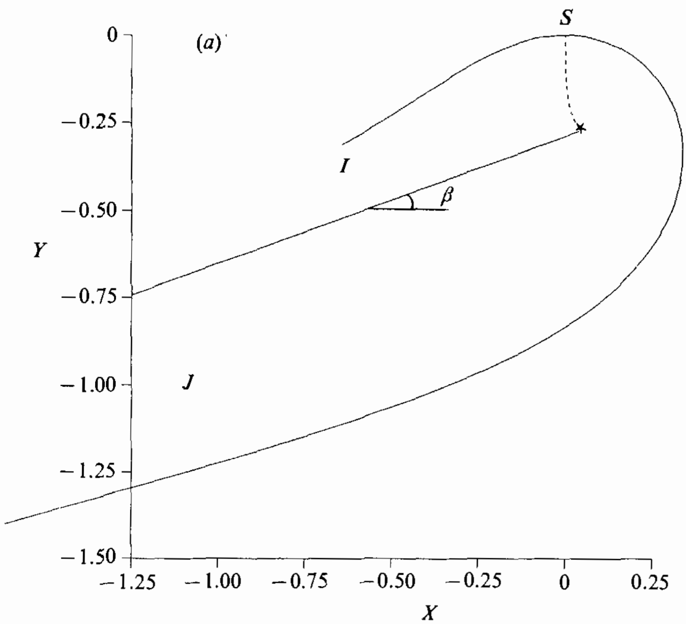

FIGURE 5(a). For caption see facing page.

used for solving the system. The integrations required to compute y_1 and y_3 were performed with the IMSL routine DQDAGS. The coefficients a_n in the power series (16) were found to decrease like n^{-2} with increasing n. Most of the computations were performed with $N = 60$.

Once this system is solved, α (i.e. the amount of fluid falling along the underside of the nozzle) is obtained from (6) and the profile of the free surface is calculated by

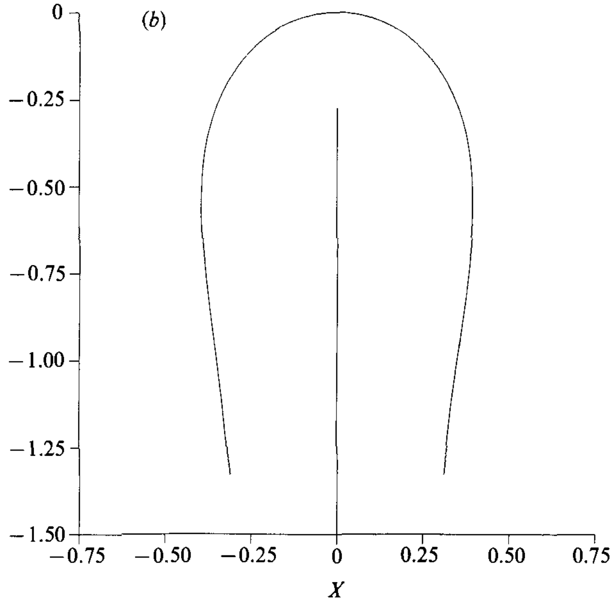

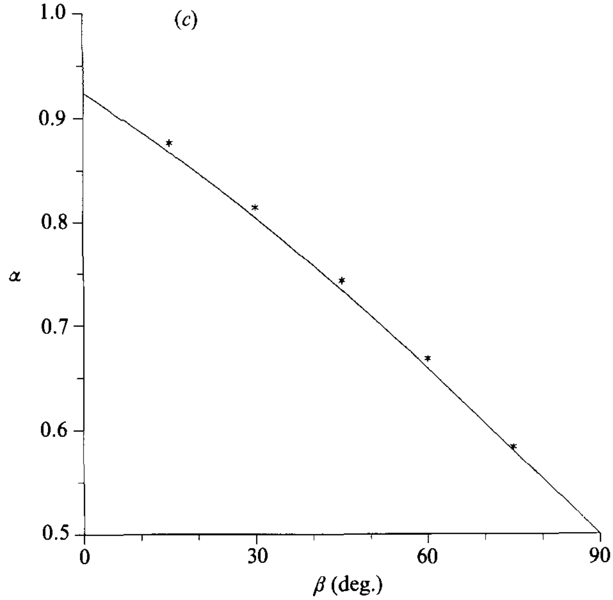

FIGURE 5. (*a*) Computed free-surface flow due to a source at the top of a wall with $\beta = 20°$. The solid curves correspond to the free surface and the wall. The position of the source is indicated by a star. The broken line is the dividing streamline. 85% of the flow goes to the right. (*b*) Same as (*a*) with $\beta = 90°$. (*c*) Values of the amount α of water falling down on the right versus the inclination β (with the horizontal) of the wall on top of which the source is located. The stars indicate the values of α obtained from figure 4 for $F = 100$.

integrating numerically (9) along the unit circle. Of interest also is the dividing streamline which terminates at S and which corresponds to the line $\psi = \psi(S)$, $\phi \leqslant \phi(S)$ in the $[f]$-plane. Equation (5) can be integrated to give

$$f = \frac{1}{\pi}\ln\left(\frac{2\mathrm{i}t\sin\gamma}{t^2-1}\right) - \frac{1}{\pi}\cos\gamma\ln\left[\mathrm{i}\tan\frac{\gamma}{2}\left(\frac{t+1}{t-1}\right)\right]. \tag{19}$$

Since (19) cannot be solved exactly to give t in terms of f, Newton's method was used to solve for t in terms of f. Given some ϕ and taking $\psi = 0$ along the dividing streamline, the problem is to find t satisfying $\phi = f(t)$. If t^n is the nth iterate, the next iterate is obtained from

$$t^{n+1} = t^n - \frac{f(t^n)-\phi}{\mathrm{d}f/\mathrm{d}t(t^n)}. \tag{20}$$

The number of iterations required to find t to an accuracy of 10^{-3} was 2 or 3.

Typical profiles are shown in figures 2 and 3. In figure 4, we present values of α versus F for different inclinations β of the nozzle. For all values of β between 0 and $\frac{1}{2}\pi$, solutions with two jets are possible. When $\beta = \frac{1}{2}\pi$, α is always $\frac{1}{2}$ because of symmetry. For $0 \leqslant \beta < \frac{1}{2}\pi$, as F decreases, α increases until it reaches 1. When $\alpha = 1$, the whole fluid falls down along the underside of the nozzle and the stagnation point S coincides with the extremity 1 of the nozzle. This limiting configuration is studied in detail in §4. As $F \rightarrow \infty$, α approaches a constant value which depends on β. Furthermore, the distance between the top of the free surface and the extremities of the nozzle tends to infinity. This suggests that as $F \rightarrow \infty$ the flow approaches the flow due to a source placed at the top of an inclined wall. This conjecture is confirmed by the calculations presented in the next section.

3. Flow due to a source

As $F \rightarrow \infty$, the solutions of §2 approach the flow due to a source of strength Q placed at the top of an inclined wall (see figure 5a). We shall extend the procedure described in §2 to calculate these limiting flow configurations.

First we introduce dimensionless variables by taking $(Qg)^{\frac{1}{3}}$ as the unit velocity and $(Q^2/g)^{\frac{1}{3}}$ as the unit length. In these variables, Bernoulli's equation (4) becomes

$$\tfrac{1}{2}(u^2+v^2)+(y\sin\beta - x\cos\beta) = \text{constant on free surface.} \tag{21}$$

The flow configuration in the $[f]$-plane is the same as in figure 1(b) with the points 1 and 3 at $\phi = -\infty$. As before we map the $[f]$-plane onto the upper half of the unit disk in the $[t]$-plane by using the transformation (5). The complex $[t]$-plane is the same as in figure 1(c) with $t_1 = t_3 = 0$ (i.e. with the points 1, 2, 3 at the origin).

Since there is a source at $t = 0$, the complex velocity ζ must have a singularity at this point. The appropriate singularity is

$$\zeta \sim \frac{1}{t^2} \quad \text{as} \quad t \rightarrow 0. \tag{22}$$

In addition, ζ must satisfy the relations (13) and (14). Therefore, we write ζ as

$$\zeta = \mathrm{i}(1+t^2-2t\cos\gamma)\left(\frac{1}{t^2}\right)\frac{[-\ln c(1-t^2)]^{\frac{1}{3}}}{[-\ln c]^{\frac{1}{3}}}\exp\left(\sum_0^\infty a_n t^n\right). \tag{23}$$

The coefficients a_n and the constant γ are to be found for a given value of the inclination β. We truncate the infinite series after $N-2$ terms and satisfy (21) at the collocation points (17). This leads to $N-1$ nonlinear equations for the $N-1$ unknowns $a_n (0 \leqslant n \leqslant N-3)$ and γ. This system is solved, as before, by Newton's method.

Typical profiles for $\beta = 20°$ and $\beta = 90°$ are shown in figures 5(a) and 5(b). Flows due to submerged sources or sinks have been calculated by previous investigators (Tuck & Vanden-Broeck 1984; Hocking 1985; Vanden-Broeck & Keller 1987a;

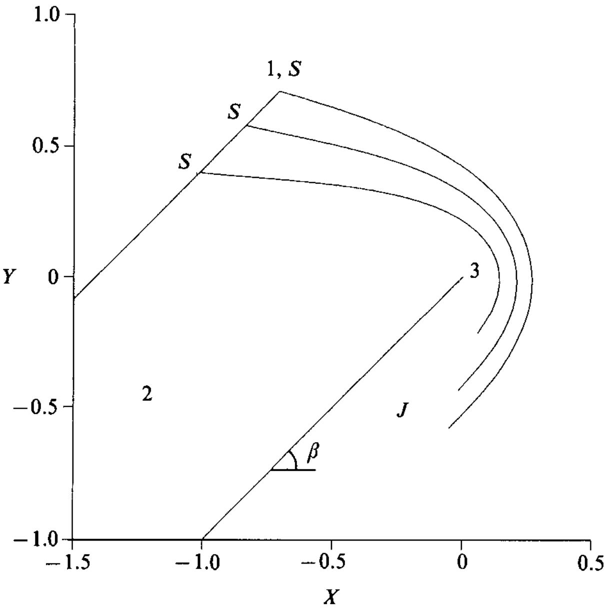

FIGURE 6. Profiles of the free surface for successive values of the Froude number. In this particular example, $\beta = 45°$ and, from top to bottom, $F = 0.63, 0.45, 0.25$.

Mekias & Vanden-Broeck 1989). The profile shown in figure 5(*b*) for a vertical nozzle is in good agreement with the profile shown in figure 8 in Mekias & Vanden-Broeck. The scaling is different in Mekias & Vanden-Broeck because the strength of their source is twice ours. Since the unit length is $(Q^2/g)^{\frac{1}{3}}$, the scaling ratio is $4^{\frac{1}{3}} \sim 1.59$. Figure 5(*c*) shows a plot of α versus β and a comparison with the values of α obtained for $F = 100$ in the previous section (i.e. for large Froude numbers in figure 4). The agreement is good for all values of β. This constitutes a check on the validity of our calculations. When the nozzle is horizontal, α is maximum but slightly less than 1.

4. Flows for which the fluid falls down along the underside of the nozzle

In this section, we consider flows which fall down along the underside of the nozzle (see figure 6). We require the stagnation point S to be below the extremity 1 of the nozzle along the side $(1, 2)$. As in §2, we use L as the unit length and U as the unit velocity. In the $[f]$-plane, the flow region is the strip $-1 < \psi < 0$ with the streamline $(2, 3, J)$ on $\psi = -1$ and the streamline $(2, S, J)$ on $\psi = 0$. We map it onto the upper half of the unit disk in the $[t]$-plane by the transformation (5) with the choice $\gamma = \pi$. The image of the stagnation point S in the $[t]$-plane is -1 (see figure 1*c*).

The appropriate singularity for ζ at the stagnation point is

$$\zeta \sim (t+1)^{\tau} \quad \text{as} \quad t \to -1, \tag{24}$$

where
$$\tau = \frac{2\beta}{\pi} \quad \text{if} \quad \tfrac{1}{3}\pi \leqslant \beta \leqslant \tfrac{1}{2}\pi \quad \text{and} \quad \tau = \tfrac{2}{3} \quad \text{if} \quad 0 \leqslant \beta \leqslant \tfrac{1}{3}\pi. \tag{25}$$

Relation (24) expresses the fact that the free surface is horizontal at S when $\frac{1}{3}\pi \leqslant \beta \leqslant \frac{1}{2}\pi$ and forms an angle of $\frac{2}{3}\pi$ with the wall of the nozzle when $0 \leqslant \beta \leqslant \frac{1}{3}\pi$. This result can be derived by using an argument similar to Stokes' argument showing that the angle at the crest of the highest progressive wave must be $\frac{2}{3}\pi$ (see Dagan & Tulin 1972 for details).

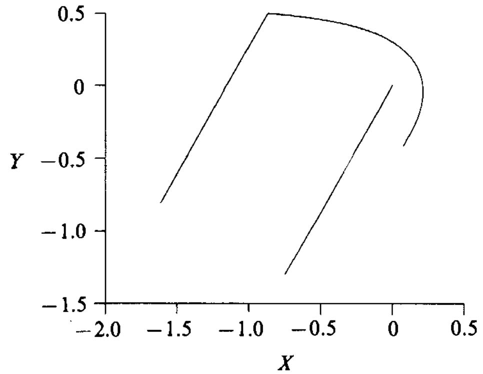

FIGURE 7. Computed free-surface flow with $\beta = 60°$ and $F = 0.39$. The stagnation point coincides with one of the extremities of the nozzle.

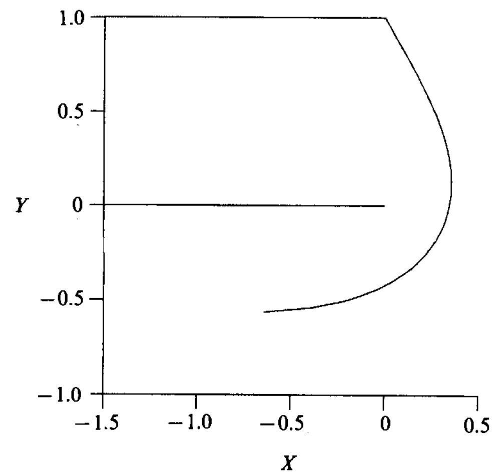

FIGURE 8. Same as figure 7 with an inclination $\beta = 0°$ and $F = 1.05$.

The singularity at 3 is given by (12). At J, there is a jet-type singularity

$$\zeta \sim [-\ln(1-t)]^{\frac{1}{3}} \quad \text{as} \quad t \to 1. \tag{26}$$

We now write the complex velocity ζ as

$$\zeta = \mathrm{i}(1+t)^{\tau}\left(\frac{1-tt_3}{t-t_3}\right)\frac{[-\ln c(1-t)]^{\frac{1}{3}}}{[-\ln c]^{\frac{1}{3}}}t_3 \exp\left(\sum_1^{\infty} a_n t^n\right). \tag{27}$$

All the equations in §2 that contain γ still hold, with γ replaced by π. The collocation procedure described in the previous sections was used to find the coefficients a_n. The numerical calculations show that there is a two-parameter family of solutions. The two parameters are β and F. In the numerical computations, it is more convenient to fix t_3 and β (instead of F and β) and to find F as one of the unknowns.

Figure 6 shows a succession of profiles of the free surface for $\beta = 45°$ and various values of the Froude number. As F decreases, the free surface becomes flatter and flatter above the nozzle.

It is interesting to study in more detail the limiting configuration in which the stagnation point S coincides with the point 1. This case can also be viewed as the

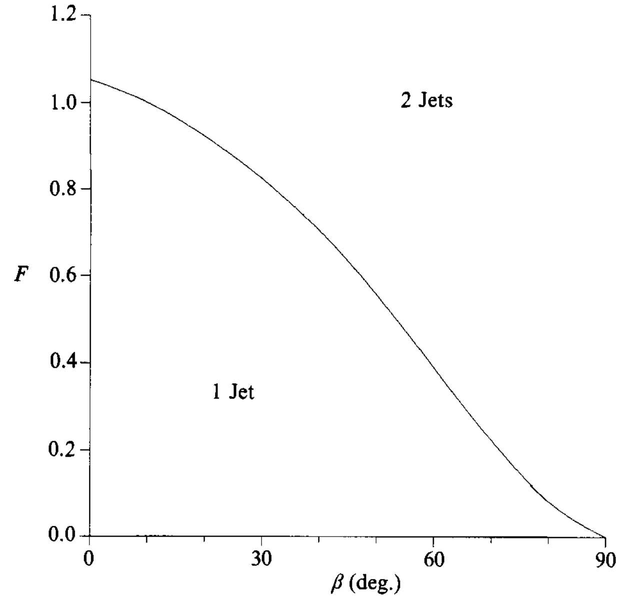

FIGURE 9. Values of the Froude number F versus the inclination β of the nozzle with the horizontal. The curve $F = F(\beta)$ separates the (β, F)-plane into two regions: the region above the curve corresponds to the solutions with two jets while the region below the curve corresponds to the solutions with only one jet.

limiting configuration of the flow studied in §2 as $\alpha \rightarrow 1$. In order to obtain these solutions, we add the constraint that the stagnation point S and the extremity 3 of the nozzle have the same y, i.e. $y(-1) = y(t_3)$. Therefore there is one less parameter. The problem is now to find the N unknowns $t_3, a_n (1 \leqslant n \leqslant N-2)$ and F, for a given inclination β of the nozzle. Thus $N-1$ mesh points are introduced along the free surface, the last equation being obtained from $y(-1) = y(t_3)$.

Figures 7 and 8 show typical profiles. Figure 9 shows the value of F versus the inclination of the nozzle β. This curve $F(\beta)$ separates the (β, F)-plane into two regions: the region above the curve corresponds to solutions with two jets and the region below to solutions with only one jet.

5. Low-Froude-number flows viewed as a combination of two pouring flows

In this section, we consider vertical nozzles, although the following considerations could be generalized for inclined nozzles. In the previous section, we observed that the free surface is rather flat above the nozzle when the Froude number is sufficiently small. This suggests that the solutions as $F \rightarrow 0$ can be described near the lips of the nozzle by the 'pouring flows' calculated by Vanden-Broeck & Keller (1986). These pouring flows are flows over a thin wall or weir with one free surface. Some pouring flows corresponding to a thin vertical wall at $x = 0$ are shown in figure 10.

Vanden-Broeck & Keller (1986) used the unit length $(\tilde{Q}^2/g)^{\frac{1}{3}}$ where $\tilde{Q}$ denotes the discharge of the pouring flow. Since the unit length used in §2 was L, we need to rescale the pouring flow solutions of Vanden-Broeck & Keller in order to compare

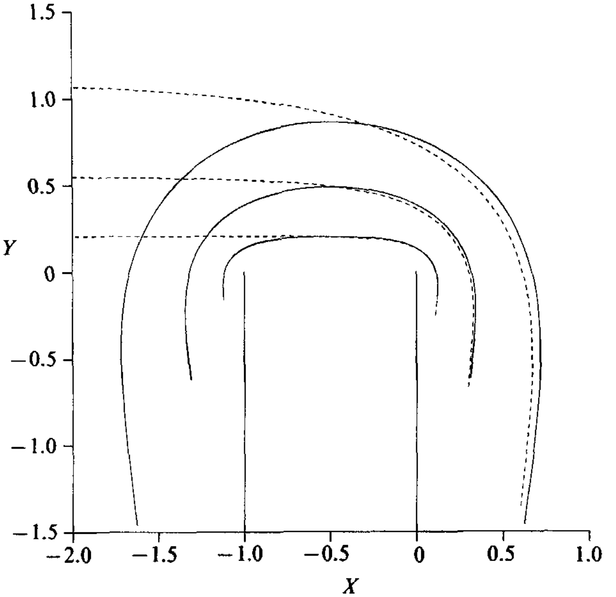

FIGURE 10. Comparison of the exact solution for the flow emerging from a nozzle with pouring flows for various values of the Froude number. The solid lines correspond to the solutions described in §2. From top to bottom, $F = 2.71, 0.94, 0.21$. The dashed lines correspond to scalings of the pouring flow solution of Vanden-Broeck & Keller (1986) by $(\frac{1}{2}F)^{\frac{2}{3}}$.

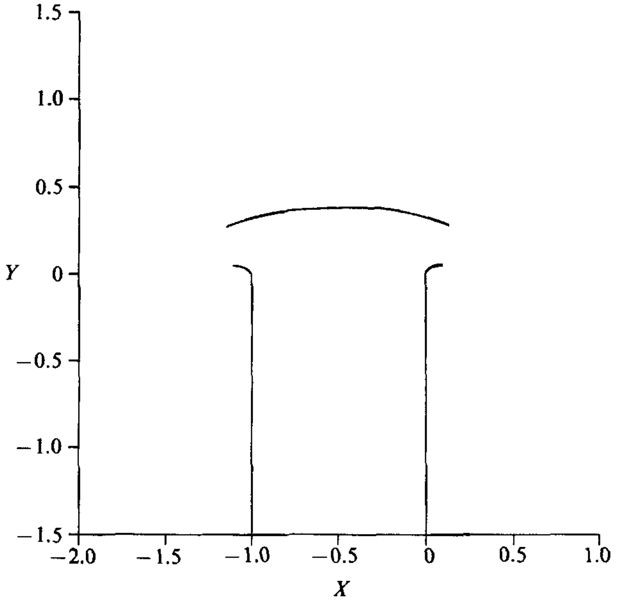

FIGURE 11. Solution with two jets each with two free surfaces obtained from the superposition of two thin weir flows for $F = 0.27$.

them with the solutions of §2 for F small. Using (1) and (2) and the fact that $\tilde{Q} = 2Q$, it is easy to show that the appropriate scaling is

$$X = \tilde{X}(\tfrac{1}{2}F)^{\frac{2}{3}} \quad \text{and} \quad Y = \tilde{Y}(\tfrac{1}{2}F)^{\frac{2}{3}}, \tag{28}$$

where $\tilde{X}$ and $\tilde{Y}$ represent the dimensionless variables used by Vanden-Broeck & Keller.

In figure 10, we present three solutions for a vertical nozzle calculated by the scheme of §2 (solid curves). They correspond from top to bottom to $F = 2.71, 0.94, 0.21$. The three broken curves are the pouring flow solutions rescaled with (28). The results show that the pouring flow provides an accurate description of the flow near a lip even for relatively large values of the Froude number. Moreover, for $F \leqslant 0.21$, the pouring flow agrees with the exact numerical solution for all values of $x > -0.5$ (see figure 10). Therefore, for F sufficiently small, the complete free surface can be obtained by superposing two pouring flows or more precisely a pouring flow and its mirror image.

Vanden-Broeck & Keller (1986, 1987*b*) also calculated pouring flows with two free surfaces (these solutions describe the flow over a thin weir). The results presented in this section suggest that these pouring flows with two free surfaces can be superimposed to generate new solutions of the nozzle problem for F small. In figure 11, we present such a solution for $F = 0.27$. It was obtained by using the thin-weir solution of Vanden-Broeck & Keller (1987*b*) (see their figure 4) and by rescaling it by (28). It is a solution with two jets each with two free surfaces. The falling parts of the jets are not shown.

REFERENCES

BIRKHOFF, G. & CARTER, D. 1957 *J. Math. Mech.* **6**, 769.
DAGAN, G. & TULIN, M. P. 1972 *J. Fluid Mech.* **51**, 529.
GOH, K. H. M. & TUCK, E. O. 1985 *J. Engng Maths* **19**, 341.
HOCKING, G. C. 1985 *J. Austral. Math. Soc.* B **26**, 470.
MEKIAS, H. & VANDEN-BROECK, J.-M. 1989 *Phys. Fluids* A **1**, 1694.
TUCK, E. O. 1987 *J. Fluid Mech.* **176**, 253.
TUCK, E. O. & VANDEN-BROECK, J.-M. 1984 *J. Austral. Math. Soc.* B **25**, 443.
VANDEN-BROECK, J.-M. & KELLER, J. B. 1986 *Phys. Fluids* **29**, 3958.
VANDEN-BROECK, J.-M. & KELLER, J. B. 1987*a* *J. Fluid Mech.* **175**, 109.
VANDEN-BROECK, J.-M. & KELLER, J. B. 1987*b* *J. Fluid Mech.* **176**, 283.